Climate Dynamics (2001) 17: 589–599

E. Guilyardi · G. Madec · L. Terray

The role of lateral ocean physics in the upper ocean thermal balance of a coupled ocean-atmosphere GCM

Received: 24 January 2000 / Accepted: 11 September 2000

Abstract The sensitivity of the upper ocean thermal balance of an ocean-atmosphere coupled GCM to lateral ocean physics is assessed. Three 40-year simulations are performed using horizontal mixing, isopycnal mixing, and isopycnal mixing plus eddy induced advection. The thermal adjustment of the coupled system is quite different between the simulations, confirming the major role of ocean mixing on the heat balance of climate. The initial adjustment phase of the upper ocean (SST) is used to diagnose the physical mechanisms involved in each parametrisation. When the lateral ocean physics is modified, significant changes of SST are seen, mainly in the southern ocean. A heat budget of the annual mixed layer (defined as the "bowl") shows that these changes are due to a modified heat transfer between the bowl and the ocean interior. This modified heat intake of the ocean interior is directly due to the modified lateral ocean physics. In isopycnal diffusion, this heat exchange, especially marked at mid-latitudes, is both due to an increased effective surface of diffusion and to the sign of the isopycnal gradients of temperature at the base of the bowl. As this gradient is proportional to the isopycnal gradient of salinity, this confirms the strong role of salinity in the thermal balance of the coupled system. The eddy induced advection also leads to increased exchanges between the bowl and the ocean interior. This is both due to the shape of the bowl and again to the existence of a salinity structure. The lateral ocean physics is shown to be a significant contributor to the exchanges between the diabatic and the adiabatic parts of the ocean.

E. Guilyardi (✉) · L. Terray
CERFACS, Toulouse, France
E-mail: ericg@lodyc.jussieu.fr

G. Madec
LODYC, Paris, France

1 Introduction

Due to its high thermal inertia and to its opacity, the ocean stores vast amounts of energy, away from a direct contact with the atmosphere. As part of the thermodynamical machine of climate, the ocean acts as a heat regulator. This regulation involves both air-sea (and ice-sea) heat exchanges and mixing within the ocean. It is therefore closely related to the internal structure of the ocean: water masses and thermocline waters are *formed* in the surface diabatic region of the ocean, are advected adiabatically, and are finally *consumed* by the only diabatic process within the ocean: turbulent mixing. Here, we wish to assess the sensitivity of the climate modelled by a coupled ocean-atmosphere GCM to the representation of such ocean physics. Our particular focus is on the role of the lateral ocean physics on the thermal balance of the upper ocean.

Classical views of the thermocline ventilation (Luyten et al. 1983) propose a theoretical framework to explain the observed density structure at mid-latitudes. This advective approach has proven successful in several regions of the ocean (Luyten et al. 1983; Rhines and Young 1982; Marshall and Nurser 1992). Nevertheless, air-sea fluxes are usually not taken into account explicitly but through the specification of the density at the base of the mixed-layer. In addition, mixing is usually neglected because it is considered small. Tziperman (1986) showed that these two simplifications are intimately related. He re-introduced mixing by showing that however small, it has a major role in the equilibrium of the thermocline. The basic physical idea underlying this approach (Walin 1982) is quite simple: air-sea implied buoyancy can generate a *net* water volume of a particular density class ρ. If the ocean is close enough to a statistically steady state, there must be a counterbalancing interior diapycnal mixing.

Many sensitivity studies have shown that the circulation of forced ocean models was highly sensitive to the representation of sub-grid scale mixing (England 1993;

Hirst and Cai 1994; Danabasoglu and McWilliams 1995; Maes et al. 97; England and Hirst 1997; see reviews by McWilliams 1996; Delecluse and Madec 1999). To avoid the limitations of forced ocean models, some recent studies have tackled the issue while coupling the ocean GCM to an atmosphere GCM (Hirst et al. 1996; Guilyardi 1997; Wiebe and Weaver 1999; Jackett et al. 2000). They showed significant impacts on the modelled climate, both in the ocean and the atmosphere. The present study aims at describing the details of the physical mechanisms that lead to these changes. We have chosen to focus the analysis on the SST. This field is the main signature of the upper ocean dynamics and represents the link between the deep ocean and the atmosphere.

The SST is, to a very good approximation, the temperature of the ocean mixed layer. Hence, the understanding of the impact of sub-grid scale physics on the SST requires an assessment of the heat balance of the mixed layer. During the year, the mixed layer shallows and deepens, sweeping the diabatic region of the ocean while integrating the air-sea fluxes. We define the lower boundary of this region to be the thermodynamical "bowl", following the dynamical bowl discussed by Marshall and Nurser (1992). This annual envelop of the mixed layer can be defined to be fixed in time and represents the boundary between the diabatic and adiabatic regions of the ocean (Fig. 1). The annual heat exchanges between these two regions of the ocean have to be computed through this surface rather than through the base of the seasonal mixed layer. Indeed, in summer, the mixed layer is shallow but the fluxes injected during the previous winter continue to interact with the ocean interior: the resulting waters (part of the seasonal thermocline, Fig. 1) are re-entrained in the mixed-layer the next winter and need therefore to be taken into account in the annual heat budget. In fact, the bowl represents an *annually integrated mixed layer* which allows to filter the seasonal cycle in the analysis of the heat exchanges between the atmosphere, the mixed layer and the ocean interior.

The initial adjustment phase of the coupled model (away from its observed initial state) is used because the "work" of the physical parametrisations is particularly visible during this period. In addition, understanding this departure from the observed (a classical bias of coupled models) will help reduce it and finally improve the model. In this study, we assess the sensitivity of the modelled climate to the lateral ocean physics on tracers, and in particular the role of lateral mixing on the bowl-ocean interior exchanges. Three 40-year coupled simulations are made using horizontal mixing, isopycnal mixing, and isopycnal mixing plus eddy induced advection, respectively.

Section 2 describes the coupled model and the sensitivity experiment. Section 3 compares the response of the three simulations with special emphasis on the air-sea interface. Section 4 focuses on the physical mechanisms involved in the exchanges between the bowl and the ocean interior. The climatic impact of these differences are discussed in Sect. 5 and we conclude in Sect. 6 with a summary and some directions for future work.

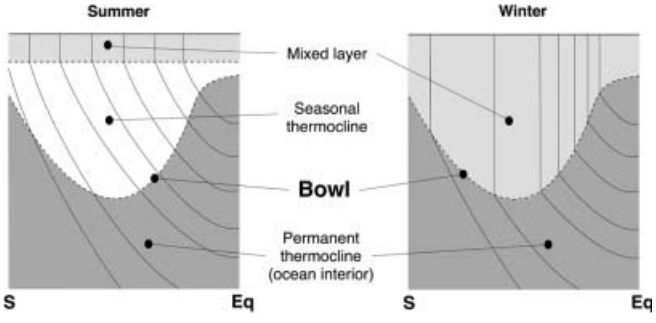

Fig. 1 Definition of the "bowl", annual envelop of the mixed-layer (*thick dashed line*). The isocontours represent the density field. The bowl is fixed in time and allows a clear distinction of the diabatic and adiabatic parts of the ocean

2 The OPA/OASIS/ARPEGE coupled model

2.1 The OPA model

The OPA8 ocean GCM has been developed at the Laboratoire d'Océanographie DYnamique et de Climatologie (LODYC) (Madec et al. 1998). It solves the primitive equations with a non-linear equation of state (Unesco 1983). A rigid lid is assumed at the sea surface. The code has been adapted to the global ocean by Madec and Imbard (1996). The horizontal mesh is orthogonal and curvilinear on the sphere. It does not have a geographical configuration: the northern point of convergence has been shifted onto Asia to overcome the singularity at the North Pole (Madec and Imbard 1996). Its space resolution is roughly equivalent to a geographical mesh of 2 by 1.5° (with a meridional resolution of 0.5° near the Equator). A total of 31 vertical levels are used with 10 levels in the top 100 m (Madec and Imbard 1996). The model time step is 1 h 40′. Vertical eddy diffusivity and viscosity coefficients are computed from a 1.5 turbulent closure scheme (Blanke and Delecluse 1993) which allows an explicit formulation of the mixed layer as well as minimum diffusion in the thermocline (the minimum background value is set to 10^{-5} m^2 s^{-1} following Ledwell et al. 1998). The solar radiation is allowed to penetrate into the top meters of the ocean (Blanke and Delecluse 1993). Zero fluxes of heat and salt and no-slip conditions are applied at solid boundaries. Sea ice is restored towards observations at high latitudes. Horizontal mixing of momentum is of Fickian type with an eddy viscosity coefficient of 4.10^4 m^2 s^{-1}, reduced in the tropics to reach 2.10^3 m^2 s^{-1} at the Equator. The lateral mixing on tracers (temperature and salinity), on which the sensitivity experiment is performed, is described in Sect. 2.4.

2.2 The ARPEGE model

The ARPEGE-climat (Version 2) atmosphere GCM, from CNRM/Météo-France, is a state of the art spectral atmosphere model developed from the ARPEGE/IFS weather forecast model (Déqué et al. 1994). The ARPEGE model used in this study is based on the version described by Guilyardi and Madec (1997) with the following differences. The model now has 19 vertical levels (with an increased resolution in the troposphere) and a triangular spectral T31 truncation is used for horizontal resolution corresponding to a 3.75° grid size. The convective entrainment rate is increased at lower levels, the radiation scheme is now based on the Fouquart-Morcrette scheme described in Dandin and Morcrette (1996) and, following Terray (1998), a parametrisation of marine strato-

cumulus is added. These last three modifications clearly improved the tropical climatology of the coupled model when compared to that of Guilyardi and Madec (1997). In particular, the strong initial tropical warming was strongly reduced (see Guilyardi 1997 for a full discussion). Finally, a 4-layer prognostic soil scheme with seasonally varying surface albedo is added as well as a new parametrisation of gravity wave drag.

2.3 Coupling procedure and initialisation

The coupling procedure is similar to the one described in Guilyardi and Madec (1997): synchronous coupling with a daily exchange of fluxes. The version 2.0 of OASIS is used (Terray et al. 1996) in which the SST of a given AGCM grid square is now the weighted average of the underlying OGCM sea grid points. The river runoffs are computed using 81 river drainage basins defined on the AGCM grid and are passed instantaneously to corresponding river mouth ocean grid points. As the analysis of the initial adjustment phase is our topic, the initial state of the ocean for each experiment is based on the atlas of Levitus (1982). From this atlas, a two-year dynamic spin-up is made in robust-diagnostic mode for each ocean physical parametrisation, which leads to the initial oceanic state of each experiment (Madec and Imbard 1996; Guilyardi and Madec 1997). No artificial flux corrections are applied at the air-sea interface (except in sea-ice covered regions).

2.4 The three sensitivity experiments

Based on the coupled model described, a sensitivity study to ocean lateral diffusion of tracer is made. A first experiment (**HOR**) is integrated for 40 years. It uses a classical horizontal harmonic diffusion scheme, with an eddy diffusivity coefficient K_H of 2000 $m^2\ s^{-1}$. As noted by many authors, this horizontal diffusion scheme generates spurious diapycnal fluxes where the isopycnals are steeply sloping. The Redi-Cox implementation of isopycnal diffusion in GFDL-type models is the classical way to overcome this problem but nevertheless requires a minimum background horizontal diffusion for numerical stability. To overcome this problem, several techniques have been proposed in which the numerical schemes of the OGCM are modified (Griffies et al. 1997; Weaver and Eby 1997). In OPA, another strategy has been chosen: the use of a *large-scale* slope (averaged over three grid points) prevents the development of grid-point noise so that no artificial background horizontal mixing has to be added (thus allowing "quasi-pure" isopycnal mixing). A 40-year coupled simulation is performed using the OPA quasi-pure isopycnal diffusion scheme (experiment **ISO**) with an eddy diffusivity coefficient K_I of 2000 $m^2\ s^{-1}$.

Baroclinic instability is a significant source of mixing within the ocean. It induces a loss of mean potential energy which is nevertheless not affected by the horizontal or the isopycnal diffusion operators. In order to mimic this process, Gent and McWilliams (1990, GM90 thereafter) proposed a quasi-adiabatic parametrisation in which an eddy induced advection is added to the tracer equation (Gent et al. 1995). This eddy induced velocity (EIV) represents the ageostrophic part of the motion (Lazar et al. 1999), in the sense that it is not in equilibrium with a pressure gradient, even though the eddies modelled (because not resolved by climate models) may be geostrophic. The eddy induced velocity proposed by GM90 is proportional to the gradient of the slope of the isopycnal ($U^* = K_{eiv}\nabla\cdot$[slope]) and therefore tends to slump density fronts. The third 40-year simulation (experiment **ISOG**) includes such an eddy induced advection, in addition to the isopycnal diffusion, with $K_{eiv} = K_I = 2000\,m^2\,s^{-1}$. This value of K_{eiv} is quite high for most ocean regions when compared to those estimated in the literature (Visbeck et al. 1997). It is nevertheless kept to 2000 $m^2\ s^{-1}$ to magnify its effect in the model. The surface boundary condition of U^* was not discussed by GM90 and is not straightforward to choose (Tréguier et al. 1997; Marshall 1997). In this first implementation of GM90 in OPA, the slopes are bounded by 1/100 everywhere, this limit linearly decreasing to zero between 70 m depth and the surface (the fact that eddies "feel" the surface motivates this flattening of isopycnals near the surface).

3 The coupled response

This section briefly describes the main differences between the three simulations, with a special emphasis on the initial adjustment phase of the air-sea interface. A more detailed assessment of the compared climatology of the three simulations can be found in Guilyardi (1997).

The zonal mean temperature change in the atmosphere after 40 years presents a similar pattern for the three simulations (Fig. 2): tropical tropospheric cooling associated to a warming at higher latitudes, especially marked in the Southern Hemisphere. Nevertheless, the magnitude of the temperature drift is significantly affected by the changes in lateral ocean physics (roughly $+2$ °C in the near surface layers from **HOR** to **ISOG** around 60°S). In contrast, the change of lateral ocean physics only very slightly affected the dynamics of the atmosphere: similar SST gradients led to similar pressure patterns and the dynamical forcing of the ocean (i.e. Ekman pumping) is quite comparable between the three simulations (not shown). The excess of heat entering the southern ocean near 50°S is diffused horizontally in **HOR** (Fig. 2a) while it remains along isotherms (isopycnals) in **ISO** (Fig. 2b), diving to 1000m. In **ISOG**, the warming signal is shallower (600 m deep at 45°S) and is spread in the surface layers by the slumping of the meridional fronts (Fig. 2c).

The zonal mean heat flux, fresh water flux and wind stress components of **HOR**, **ISO** and **ISOG** displayed in Fig. 3 are quite close to each other when compared to climatology. The main common bias are extra-tropical: higher-than-observed heat fluxes entering the ocean at mid-latitudes (Fig. 3a) (mostly due to a lack of clouds and deficient turbulent fluxes in the atmosphere GCM) and quite strong westerlies, especially over the Southern Ocean (Fig. 3c). Most of the differences between the three simulations are found south of 40°S. They mainly concern the heat flux entering the ocean (which diminishes between 40°S and 60°S from **HOR** to **ISO** and to **ISOG**) while the freshwater flux and wind stress undergo very little changes.

The annual-mean SST of all 3 simulations increases from their common initial state (Fig. 4). This common feature is due to the atmosphere GCM deficiency discussed above, which generates higher-than-observed heat flux for most extra-tropical latitudes (Fig. 3a). Nevertheless, the *amplitude* and the *time scale* of the SST warming are strongly affected by the change in lateral ocean physics: the annual-mean SST of **HOR** increases slowly but steadily while the initial increase in **ISO** is much stronger but reaches a quasi-equilibrium for the last 20 years of the simulation (Fig. 4). The annual-mean SST of **ISOG** exhibits the same behavior as the

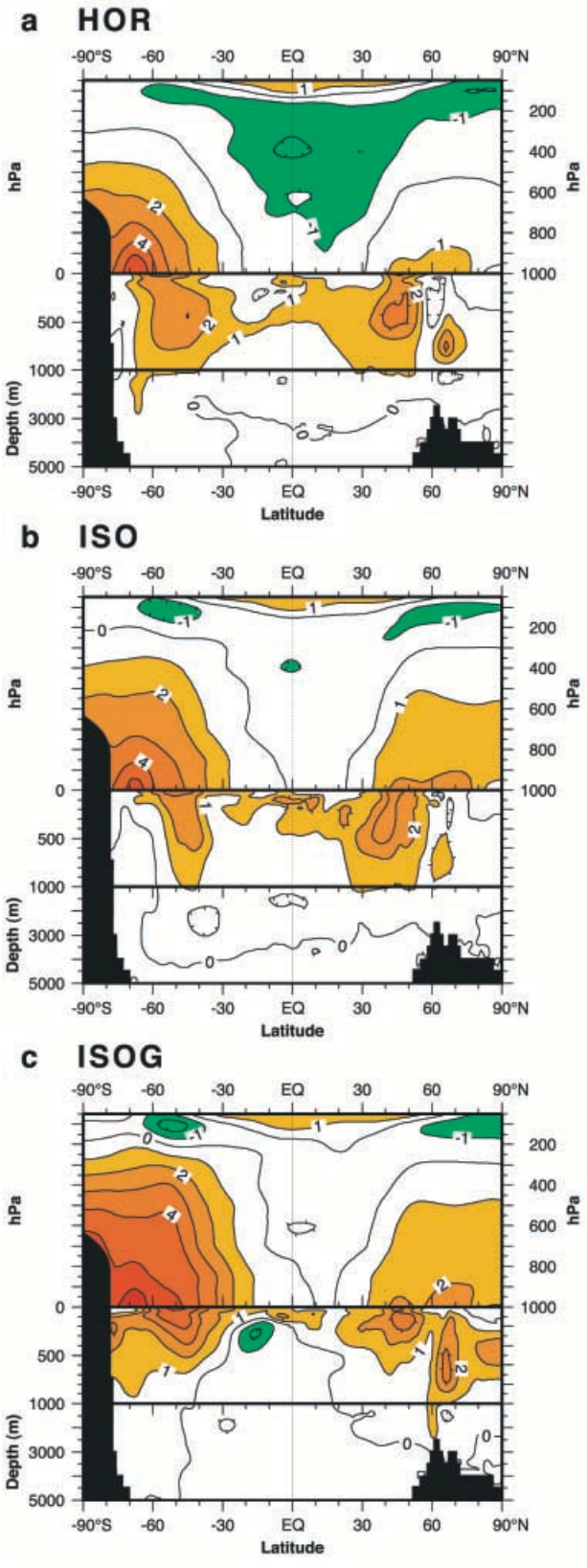

Fig. 2a–c Zonal mean temperature (°C) in the coupled ocean-atmosphere system. Differences with the initial state (Levitus) of each simulations of the average of years 26–40. **a** Simulation **HOR**, **b** simulation **ISO**, **c** simulation **ISOG**. Contour interval 1 °C. *Light shading* for cooling and *darker shading* for warming

one of **ISO**, the initial warming during the first 3 to 5 years being even stronger. This faster adjustment time of **ISOG** is consistent with the analysis of Weaver and Wiebe (1999). Global SST differences after 40 years are close to 1 °C, suggesting significant changes in the initial thermal adjustment of the coupled model.

Difference maps after three years show that most of the SST differences occur at mid-latitudes, where the isopycnals have the strongest slope (Fig. 5). In particular, the SST warming from **HOR** to **ISO**, and further from **ISO** to **ISOG**, mostly takes place in the southern ocean where differences up to 3 °C are locally seen (Fig. 5a). After 40 years, the patterns and amplitude of SST differences are similar to the first three years (not shown), as expected from Fig. 4. A first candidate to account for these SST differences is a change of downward heat flux at the air-sea interface. For the first three years, the net heat fluxes entering the ocean for **HOR**, **ISO** and **ISOG**, are 7, 5.5 and 4 W m^{-2}, respectively (these figures stabilising to 4.2, 3.5 and 1.5 W m^{-2}, respectively, after 40 years). This indicates that the heat flux is not responsible for the SST increase from one simulation to the other. This reduced heat flux, mostly due to the latent heat flux (not shown) and located in the southern ocean (Fig. 3a) is actually a response to the increase of SST. Moreover, the other atmospheric boundary layer fields of each experiment are quite similar (wind stress curl, etc... – not shown). Hence, the heat required to increase the SST from **HOR** to **ISO** and further from **ISO** to **ISOG** must come from the ocean interior: an investigation of the thermal balance in the ocean is needed.

4 The heat balance of the bowl

The SST is, to a very good approximation, the temperature of the ocean mixed layer. Hence, in order to understand the SST differences described, we need to assess the heat balance of the bowl defined as the annual (or multi-annual) envelop of the mixed layer (see Introduction).

The bowl is defined for each simulation as the maximum depth reached by the mixed layer over the study period. As we wish to assess the compared initial adjustments, this study period is first defined as years 01-02-03. For each simulation, the bowl is a fixed surface in time. As the ocean structures of the three simulations are still close to each other, the three bowls are similar and allow easier comparison. The bowl temperature balance is also assessed for years 38–40. Using either the bowl constructed from years 01–03 or the one constructed from years 38–40 does not change the results qualitatively.

The mixed layer used to define the bowl for each simulation is computed using a thermodynamical criterion on density ($\rho < \rho_0 + 0.01$, where ρ_0 is the surface density) rather than a dynamical criterion built on the intensity of the vertical mixing (“turbocline”). In the remainder of the work, the bowl is to be understood as

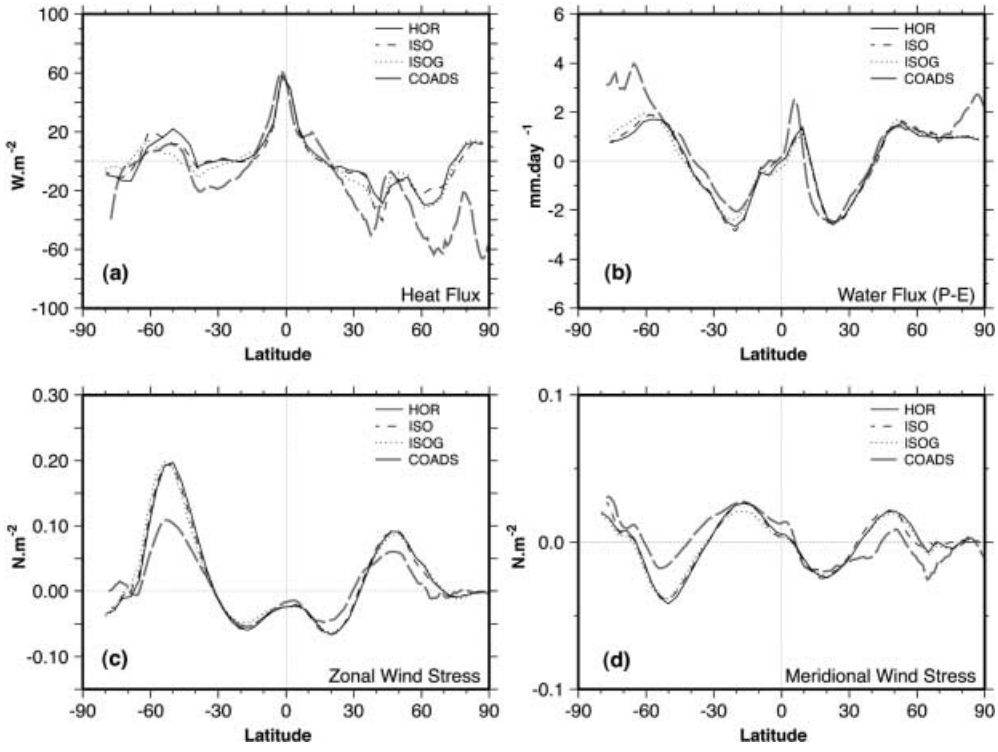

Fig. 3a–d Zonal mean of air-sea fluxes. Average of years 26–40 for simulations **HOR-ISO-ISOG**; COADS climatology by Da Silva et al. 1996. **a** Downward heat flux, **b** freshwater flux ($P - E$), **c** zonal wind stress and **d** meridional wind stress

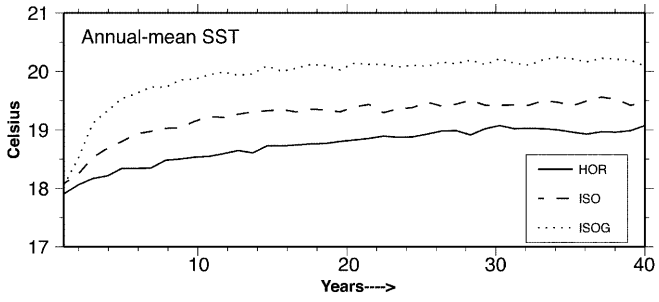

Fig. 4 Time evolution of the annual-mean global SST (°C) for the three simulations **HOR-ISO-ISOG**

the *volume* between the surface and the bowl defined above.

4.1 Heat balance computation

The different tendencies driving the temperature equation in the bowl are vertically integrated at each time step for the first three years of each simulation, leading to the following equation (Vialard and Delecluse 1998):

$$\frac{\partial T_{\mathrm{bowl}}}{\partial t} = \mathbf{Adv} + \mathbf{Forc} + \mathbf{SGS} \qquad (1)$$

where $T_{\mathrm{bowl}} = (1/H)\int_{-H}^{0} T\,\mathrm{d}z$ is the bowl temperature, H being the depth of the bowl, **Adv** is the advective trend, **Forc** is the trend due to the forcing (air-sea fluxes) and **SGS** is the trend associated with sub-grid-scale processes. This last term includes the tendency due to the lateral diffusion $\mathbf{Diff}_l$ (horizontal for **HOR** and isopycnal for **ISO** and **ISOG**), the vertical diffusion $\mathbf{Diff}_v$ and, for **ISOG**, to the eddy induced velocity $\mathbf{Adv}_{eiv}$.

The cumulated tendencies in a southern region located where the difference maxima between the simulations occur (box 130°E-80°W-40°S-65°S drawn in Fig. 5a) are presented for the three simulations and for the three first years in Table 1.

The basic balance in **HOR** at this latitude is between the forcing (warming, Fig. 3a) and the advection (cooling by Ekman drift, Fig. 3c), the other terms being small (Table 1). In **ISO**, the increase of T_{bowl} (+0.3 °C/year when compared to **HOR**) is solely due to the lateral diffusion $\mathbf{Diff}_l$ (+0.64 °C/year), i.e. the effect isopycnal diffusion, all the other terms tending to counterbalance this warming. The strong additional warming from **ISO** to **ISOG** (+0.28 °C/year) is also only due to the added physics: the eddy-induced advection $\mathbf{Adv}_{eiv}$ adds 1.06 °C/year to the bowl, while the other terms (forcing and advection mostly) again tend to counter balance this effect (Table 1). After 40 years, the bowl heat budgets of **HOR**, **ISO** and **ISOG** exhibit the same relative balance between the tendencies as during the initial years (not shown) except that a quasi-equilibrium of T_{bowl} is reached for all three simulations ($\partial_t T_{\mathrm{bowl}} \sim 0.01$ °C/year) due to a decrease of the forcing term. Hence, most of the conclusions regarding the behaviour of the different lateral physics can be obtained from the first three years of simulation.

The warming due to $\mathbf{Diff}_l$ in **ISO** (and to $\mathbf{Adv}_{eiv}$ in **ISOG**) is active all year long, but exhibit a marked maximum at the end of the winter, when the mixed-layer fully occupies the bowl, i.e. when the ocean interior is in direct contact with the atmosphere via the mixed-layer

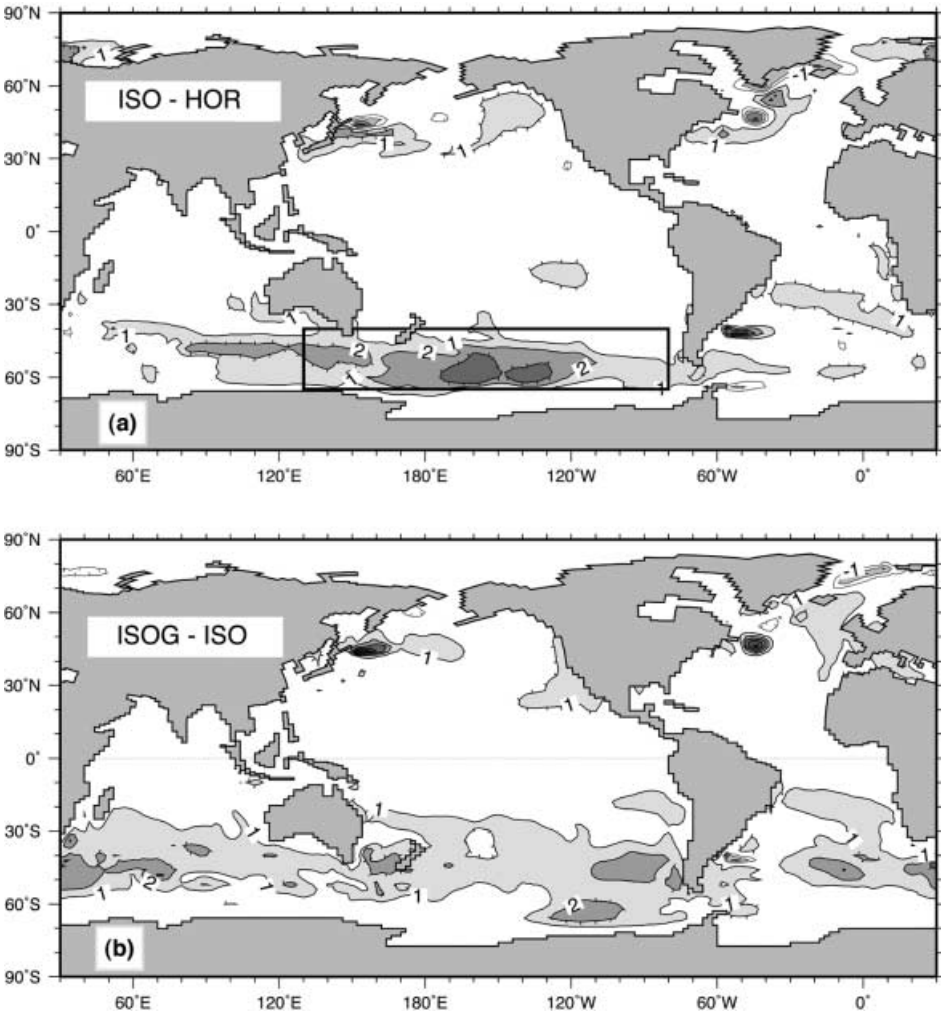

Fig. 5a, b SST differences for year 03 (°C). **a ISO** minu **HOR** and **b ISOG** minus **ISO**. Contour interval 1 °C

Table 1 Bowl temperature tendencies (°C/year) integrated for years 01-02-03 of simulations **HOR-ISO-ISOG** in the region 130°E–80°W–40°S–65°S, and differences. $\partial_t T_{\mathrm{bowl}}$ is the total trend; **Forc** the forcing trend; **Adv** the advection trend; $\mathbf{Diff}_l$ and $\mathbf{Diff}_v$ the lateral and vertical diffusion tendencies and $\mathbf{Adv}_{eiv}$ the eddy induced advection trend

°C/year (01-02-03)	HOR	ISO	ISOG	ISO -HOR	ISOG -ISO
$\partial_t T_{\mathrm{bowl}}$	0.17	0.47	0.75	0.30	0.28
Forc	1.03	0.96	0.74	−0.07	−0.22
Adv	−1.03	−1.25	−1.72	−0.22	−0.47
$\mathbf{Diff}_l$	0.10	0.74	0.69	**0.64**	−0.05
$\mathbf{Diff}_v$	0.07	0.02	−0.02	−0.05	−0.04
$\mathbf{Adv}_{eiv}$	–	–	1.06	–	**1.06**

(Fig. 1b). The sign of $\mathbf{Diff}_l$ in isopycnal diffusion indicates that the ocean interior is warming the bowl.

4.2 The role of salinity in isopycnal mixing

Hirst and Cai (1994) qualitatively described such heat and salt exchanges between the subsurface and the mixed-layer in a forced isopycnal simulation. Understanding and quantifying this mixed-layer heating by $\mathbf{Diff}_l$ from the ocean interior in **ISO** requires to elucidate its *sign* and its increased *magnitude* when compared to $\mathbf{Diff}_l$ in **HOR**. The isopycnal diffusion trend $\mathbf{Diff}_l$ can be written as the product of the lateral diffusion coefficient K_l, the lateral gradient of temperature $\nabla_l T$ and the effective surface of lateral diffusion S_{eff_l}, divided by the volume of the bowl V:

$$\mathbf{Diff}_l = V^{-1} \cdot K_l \cdot \nabla_l T \cdot S_{eff_l} \quad .$$

We saw that $\mathbf{Diff}_{ISO}$ is one order of magnitude larger than $\mathbf{Diff}_{HOR}$ (Table 1) although $\nabla_{\mathbf{ISO}}\mathbf{T}$ is significantly less than $\nabla_{\mathbf{HOR}}\mathbf{T}$. Table 2 shows the annual-mean components of $\mathbf{Diff}_l$ in the southern region of study for year 01 of **HOR** and **ISO**. The ratio $\mathbf{Diff}_{ISO}/\mathbf{Diff}_{HOR}$ is equal to 9.1 and is almost entirely due to the increased effective surface of lateral diffusion S_{eff_l}, which is the perpendicular projection of the diffusion direction on the surface of the bowl. Indeed, in isopycnal diffusion, the *horizontal* surface of the ocean comes into play in S_{eff_l}. Because of the strong vertical/horizontal aspect ratio of the ocean, the surface of the vertical projection of the bowl is several orders of magnitude larger than its

horizontal counterpart. This leverage effect is small in the tropics where the slope of the isopycnals is small but becomes quite important at mid-latitudes, explaining the magnitude of $\mathbf{Diff}_I$ there in **ISO**. The sign of $\mathbf{Diff}_I$ can be explained by looking at a "vertical" temperature section in the south Pacific, where depth is replaced by density (Fig. 6a). (NB. Even though tracers are diffused along neutral density surfaces, potential density is a quite good approximation in the surface layers, particularly in the Pacific Ocean, You and McDugall 1990.) This section, typical of the southern ocean structure, allows a clear view of *positive* isopycnal temperature gradients between the ocean interior and the bowl. For instance, at $\sigma_0 = 27.3$, the temperature just below the bowl is ~4 °C while it is ~2 °C inside the bowl (Fig. 6a). Following the definition of an isopycnal (neutral surface), $\nabla_I T$ is proportional to $\nabla_I S$, where S is the salinity. This confirms (and quantifies) the key role of salinity in isopycnal heat exchanges. Without salt, isopycnal mixing becomes isothermal, and the SST of **ISO** could not increase when compared to that of **HOR**. Around 40–60°S, where the maximum of $\mathbf{Diff}_I$ is seen in **ISO**, the surface salinity is quite low (Fig. 6b) (precipitations and sea-ice cycle) while the salinity of the waters just below the bowl (further down the isopycnals) is higher, due to the advection of high salinity subtropical waters by the gyre (Fig. 6b, c). Assuming $K_I = 1000\,\mathrm{m^2\,s^{-1}}$, Osborn (1997) estimated such isoneutral heat fluxes from the Levitus (1982) atlas to be about 10 to 15 W $\mathrm{m^{-2}}$ upwards at mid-latitudes, near the base of the bowl. He further shows that applying horizontal diffusion to the temperature field will generate a (spurious) diapycnal heat flux directed *downwards* in most of the ocean. These quite different effects of horizontal and isopycnal diffusion on the heat transfer near the base of the bowl are strikingly illustrated by contrasting Fig. 6a, c. In particular Fig. 6c clearly shows the strong diapycnal component of horizontal diffusion, as well as a quite different direction of diffusion across the bowl.

Table 2 Components of the isopycnal diffusion temperature trend $\mathbf{Diff}_I (= V^{-1} \cdot K_I \cdot \nabla_I T \cdot S_{eff_I})$ in the bowl of the Southern Ocean region drawn in Fig. 5

	V^{-1} 10^{-15} m^3	K_I m^2 s^{-1}	$\nabla_I T$ 10^{-5} °C m^{-1}	S_{eff_I} 10^{10} m^2
HOR	1/6.2	2000	1.6	0.9
ISO	1/5.0	2000	1.0	17
Ratio **ISO**/**HOR**	1.2	1	0.6	19

Mean values for year 01 of **HOR** and **ISO**, and ratio. See text for definitions. The order of magnitude between $\mathbf{Diff}_{HOR}$ and $\mathbf{Diff}_{ISO}$ is almost entirely due to the increase of the effective surface of lateral diffusion S_{eff_I}

4.3 The eddy induced advection effect

In **ISOG**, the warming of the bowl by $\mathbf{Adv}_{eiv}$ in the Southern Ocean region of study is due to the southward eddy induced heat transport through the base of the bowl. As implied by Fig. 2c (in particular by the position of the zero difference isocontour), more heat is transferred from lower to higher latitudes. Because of the particular shape of the bowl at the latitude of the region of study (downwards towards the south) and because of the existence of the isopycnal gradient of temperature described, $\mathbf{Adv}_{eiv}$ is a positive contribution. In the mixed-layer, the individual eddy induced and resolved-scale transports feature large and opposing heat transports (Gent and McWilliams 1996). Table 1 allows us to quantify the net heating due to these transports: in **ISOG**, $\mathbf{Adv}_{eiv}$ is warming the region of study by 1.06 °C/year while the resolved-scale advection (**Adv**) cools the region by 1.72 °C/year. The cooling by **Adv** is increased when compared to that of **ISO** (−0.47), but not enough to balance the eddy induced warming (Table 1), evidencing the expected exaggerated effect of the eddy induced parametrisation. This strong effect is due to the extreme case considered here (high and constant value of K_{eiv}). The strong southward eddy induced heat transport in the mixed-layer contributes to the strong stratification seen at the base of the bowl (the vertical density gradient there is multiplied by 3 from **ISO** to **ISOG**).

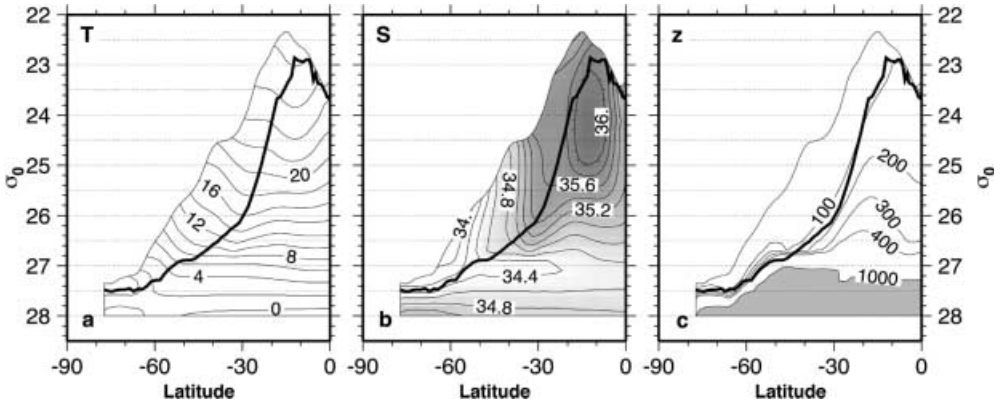

Fig. 6a–c Latitude/potential density section at 160°E in the south Pacific for march 03 of simulation **ISO**. **a** Temperature (°C), **b** salinity (PSU), **c** depth (m). The bowl of year 01-02-03 is denoted by a *thick curve*, the *thin curve* above it being the ocean surface

5 Discussion

5.1 Climatic impacts

The changes of SST from one simulation to the other have non-negligeable impacts on the simulated climate. Global-mean SST differences of the order of 1 °C after 40 years (Fig. 4) modified the air-sea heat fluxes (hence the top-of-the-atmosphere radiative balance) up to several watts per square meter. The sensitivity of the coupled system to the ocean physics is less spectacular than its sensitivity to atmosphere physics or resolution (Terray 1998; Madec and Delecluse 1997), but the choice of lateral ocean physics plays a significant role in the adjustment of long-term climate simulations (Wiebe and Weaver 1999). Indeed, the rate at which water masses and thermocline waters are transformed affects the rate at which they are formed, hence the air-sea fluxes. The change in surface heat flux appears small when compared to present-day error bars in observed fluxes (1 or 2 W m^{-2} versus 20 to 50 W m^{-2}), but one must keep in mind that the ocean integrates these differences (a heat flux of 1 W m^{-2} applied to a 100 m-deep mixed-layer raises its temperature by 1 °C in 10 years). In addition, sensitivity experiments to doubling CO_2 (Cubash et al. 1992; Mitchell et al. 1995; Barthelet et al. 1998), show changes of SST and air-sea fluxes of the same order of magnitude as the ones seen in the present sensitivity experiment and those of Hirst et al. (1996) or Wiebe and Weaver (1999). As mentioned by McDougall et al. (1996), the ocean intake of heat is quite dependent on the ocean mixing parametrisation. The "equivalent resistivity" of the bowl, which measures the resistance of the mixed-layer to an atmospheric warming Q_w, can be associated to an "equivalent heat transfer coefficient" $\mathbf{K}_{tr}$ defined by the relation:

$$Q_w = \rho_0 C_p \mathbf{K}_{tr} \frac{\langle Ta_{2m} \rangle - \langle T_{bb} \rangle}{\langle H \rangle} \quad (2)$$

where Ta_{2m} is the 2 m air temperature, T_{bb} is the temperature at the base of the bowl, H is the depth of the bowl, ρ_0 is a reference density, C_p the specific heat of seawater and where $\langle . \rangle$ indicates a global horizontal average. From $\mathbf{K}_{tr}$, we can define a characteristic time of heat transfer $\tau_{th} = \langle H \rangle^2 / \mathbf{K}_{tr}$. The values of τ_{th} computed for years 39–40 (after the initial adjustment phase of the upper ocean) for simulations **HOR**, **ISO** and **ISOG** are 30, 34 and 55 years, respectively. This indicates that the equivalent resistivity of the bowl increased by 10% from **HOR** to **ISO** and further by 60% from **ISO** to **ISOG**. We have seen in Sect. 4 that in **ISO**, additional heat was transported from the ocean interior to the bowl (when compared to **HOR**) hence increasing the characteristic time of *net* heat transfer between the diabatic part of the ocean and the adiabatic part. In **ISOG**, even more heat is given back by the ocean interior to the bowl, hence the reduced global heat intake. One might further wonder how would the bowl equivalent resistivity respond to a global *cooling* due to air-sea fluxes, rather than the warming seen here. The compared response of the three ocean physics is likely to be somewhat different as the dynamics of the mixed layer under cooling (destabilising effect) is quite different from the one under warming (stabilising effect). In the Northern Hemisphere, the net flux entering the ocean is negative (Fig. 3a) even though still warmer than observed. Nevertheless, the upper ocean dynamics and thermodynamics are significantly complicated by the gyre circulation in both the North Pacific and the North Atlantic. Hence the heat balance of the bowl in the north is quite difficult to compare to the heat balance of the bowl of southern region previously discussed. A series of coupled simulations exhibiting a surface cooling over the Southern Ocean would therefore be needed to conclude on that specific point.

The total heat transport in the Southern Hemisphere exhibits marked differences between the three simulations (Fig. 7a). In **ISO**, as no background K_H is used, the diapycnal mixing is very small and the sub-grid scale contribution to the heat transport across the Antarctic Circumpolar Current (ACC) is strongly reduced when compared to that of **HOR** (Fig. 7b). The consequence is that, even though **ISO** has an ocean density structure in better agreement with the initial state (it was not diffused away as in **HOR**), it has an unrealistic (at least with the present atmosphere GCM physics) total meridional heat

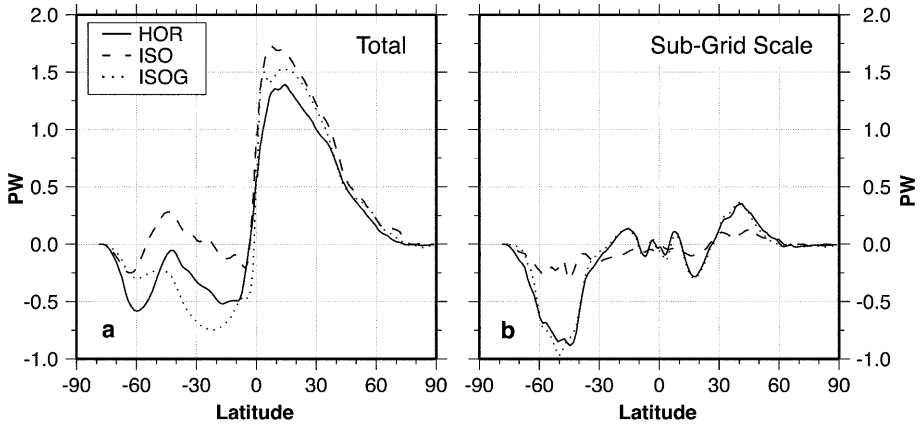

Fig. 7a, b Meridional heat transport in the ocean (PW). Average of years 26–40 for the three simulations **HOR-ISO-ISOG**. **a** Total transport, **b** transport due to sub-grid-scale processes

transport in the Southern Hemisphere. In the real world, eddies play a important role in transfering heat across the ACC. Indeed, adding an eddy induced velocity increases the SGS heat transport across the ACC in **ISOG** (Fig. 7b) and the total heat transport is now again poleward in the Southern Hemisphere (Fig. 7a). (NB. The meridional heat transport due to the eddy induced advection has the same magnitude and latitudinal distribution as the sub-grid scale transport in **HOR** (Fig. 7b). This is due to the distribution of latitudinal temperature gradients and the equivalence of the two parametrisations was shown by Lazar et al. (1999).) Moreover this is now achieved without the strong diffusive bias of **HOR**.

5.2 Interaction between physical parametrisations

Even though vertical and lateral mixing parametrisations are distinct, they both act to transform water masses. Hence, a change in one of the two is likely to affect the other. This was clearly shown by Maes et al. (1997) in the tropics where decreasing the horizontal eddy viscosity and diffusivity coefficients led to an increase of the corresponding vertical coefficients and significant changes in the equatorial circulation. In the present study, this direct link between lateral and vertical mixing is straightforward when using Walin's (1982) approach. In **HOR**, both horizontal and vertical mixing participate to water-mass transformation (through diapycnal mixing). In **ISO**, the lateral mixing is isopycnal and the only source of diapycnal mixing (away from the surface layers) is the vertical mixing scheme. As a consequence, this mixing increases to take over the diapycnal exchanges performed by the horizontal operator in **HOR**. For instance, in the ocean interior of the Northern Hemisphere, the mean vertical diffusion coefficient K_V in the thermocline ($25 < \sigma_0 < 27$) went from 0.18 10^{-4} m^2 s^{-1} in **HOR** up to 0.25 10^{-4} m^2 s^{-1} in **ISO**, a 40% increase.

A second type of interaction between parametrisations was seen in the Southern Ocean, where a change of ocean physics evidenced a physical deficiency in the atmospheric boundary layer (higher-than-observed heat fluxes). Indeed, improving the physics of the ocean degraded the SST in the Southern Ocean: in **HOR** the spurious excess of heat entering the mixed layer made its way towards the interior of the ocean faster than in **ISO** or **ISOG** (due to the weaker equivalent resistivity of the bowl). The added physics in **ISO** and **ISOG** increased the equivalent resistivity of the bowl and trapped the additional heat coming from the atmosphere GCM in the ocean surface layers. The subsequent increase of SST in turn modified the heat fluxes computed by the atmosphere GCM (decrease of the latent heat flux). But this change did not necessarily have an effect on the deficient parametrisation (clouds) in this region. This is an intricate coupled problem between ocean and atmosphere GCM parametrisations and should be tackled as such (Terray 1998).

6 Conclusion

The sensitivity of the upper ocean thermal balance of a coupled ocean-atmosphere GCM to ocean lateral physics is addressed. Three 40-year coupled simulations are made using the OPA/OASIS/ARPEGE model: **HOR** with horizontal diffusion, **ISO** with isopycnal diffusion and **ISOG** with isopycnal diffusion plus an eddy induced advection (GM90). In response to the change of ocean physics, the air-sea heat exchanges are modified by several W m^{-2} (further modifying the top-of-the-atmosphere radiative balance). This confirms the central role of ocean turbulence in the climate system: the rate at which water masses and thermocline waters are transformed affects the rate at which they are formed (Walin 1982), hence the air-sea fluxes. The initial adjustment phase of the SST is used to diagnose the physical mechanisms involved in each parametrisation. When the lateral ocean physics is modified, significant changes of SST are seen at mid-latitudes, in particular in the Southern Ocean. An excess of heat entering the ocean there is originally due to larger-than-observed atmospheric heat fluxes generated by the atmosphere GCM in this region. In **HOR**, the associated warming is diffused away in the ocean interior while part of it given back to the mixed-layer when new lateral physics are added. A measure of the rate of ocean heat intake is derived as an "equivalent resistivity of the bowl". From **HOR** to **ISO** and further to **ISOG**, this resistivity increases and the associated characteristic times of heat transfer are 30, 34 and 55 years, respectively.

The isopycnal scheme modifies the heat input from the mixed-layer into the ocean interior and is therefore directly responsible for the Southern Ocean SST increase seen from **HOR** to **ISO**. The physical mechanism responsible is a positive heat flux from the ocean interior into the mixed-layer. It is both due to an increased effective surface of diffusion across the base of the annual mixed-layer (defined as the bowl) and to the sign of the isopycnal gradients of temperature. As isopycnal gradients of temperature are proportional to isopycnal gradients of salinity, the robust mechanism evidenced in this study confirms the strong role of salinity in the heat balance of climate. Indeed, as shown here, the salinity structure strongly participates in the thermal consumption of the ocean (especially at mid-latitudes) and therefore in the heat exchanges between the ocean and the atmosphere. This result is all the more interesting as the surface coupling of salt and fresh water is quite weak when compared to that of SST and heat fluxes, allowing complex feedbacks yet to be explored.

The eddy induced advection also leads to increased exchanges between the bowl and the ocean interior. This is both due to the shape of the bowl and again to the existence of a salinity structure. The corresponding strong advective heat transfer from the ocean interior towards the bowl reduces the heat intake of the ocean interior. This effect is too strong as adding the GM90

eddy induced velocity degrades the upper-ocean structure when compared to that of **ISO**. The choice of a strong and constant eddy induced coefficient plus the particular boundary conditions chosen in the mixed-layer led to a rather extreme case of the parametrisation. An intense surface poleward heat transport led to a strong stratification at the base of the mixed-layer. Nevertheless, by allowing non-diffusive sub-grid-scale transport across horizontal gradients, the eddy induced velocity improves the meridional heat transport in the Southern Ocean, when compared to that of the isopycnal-only simulation. Eddies play an important role in transporting heat across the ACC. Here, this effect is exagerated by the particular set-up of GM90 chosen. The real transport is probably in between that of **ISO** and **ISOG** as discussed by Speer et al. (1999) who analysed the impact of eddy induced advection in the present simulations in the Southern Ocean.

The lateral ocean physics is therefore shown to be a main contributor to the exchanges between the diabatic and the adiabatic parts of the ocean (with the same magnitude as the vertical ocean physics). Hence its central climatic role, both due to a control of the heat intake capacities of the ocean and to its ability to extract long-term memory from the ocean interior towards the warm sphere of the coupled ocean-atmosphere system.

Beyond the impact on the initial adjustment of the mean state of the simulated climate, the lateral physics has an impact on its variability. The analysis of the present simulations made by Raynaud et al. (2000) shows modified ENSO dynamics with modified lateral ocean physics. Furthermore, the mid-latitudes atmosphere – ocean interior connection due to isopycnal diffusion is found all year round but has a marked maximum at the end of the winter, modifying the strong seasonal cycle of temperature there, mostly driven by forcing. This could allow a participation of the ocean interior to the low-frequency variability of the coupled system at these latitudes as well.

Acknowledgements We especially thank Kevin Speer, Olivier Thual, Pascale Delecluse, Jean-François Minster and David Marshall for helpful discussions. Maurice Imbard and Michel Déqué provided the ocean and atmosphere GCMs. Jérome Vialard helped with the computation of the tendencies in OPA8. Two reviewers provided helpful comments. This work was partially supported by EEC contract ENV4-CT95-0102 SIDDACLICH and by PNEDC (French National Program for the Study of Climate Dynamics). Computations were carried out at the computing centres of Météo-France and IDRIS/CNRS.

References

Barthelet P, Terray L, Valcke S (1998) Transient CO_2 experiment using the ARPEGE/OPAICE non-flux corrected coupled model. GRL 25–13: 2277–2280

Blanke B, Delecluse P (1993) Low frequency variability of the tropical Atlantic ocean simulated by a general circulation model with mixed layer physics. J Phys Oceanogr 23: 1363–1388

Cubash U, Hasselman K, Rock H, Maier-Reimer E, Mikolajewicz U, Santer B, Sausen R (1992) Time-dependant greenhouse warming computations with a coupled ocean-atmosphere model. Clim Dyn 8: 55–69

Danabasoglu G, McWilliams J (1995) Sensitivity of the global ocean circulation to parametrisations of mesoscale tracer transports. J Clim 8: 2967–2987

da Silva AM, Young CC, Levitus S (1994) Atlas of Surface Marine Data 1994, Volume 3: Anomalies of Heat and Momentum Fluxes. NOAA Atlas NESDIS 8, US Dept. of Commerce

Delecluse P, Madec G (1995) Ocean modelling and the role of the ocean in the climate system. In: WR Holland, S Joussaume, F David (eds) Modelling the Earth's climate and its variability. Les Houches, session LXVII 1997, Elsevier Science, Amsterdam, pp 237–313

Dandin P, Morcrette J-J (1996) The ECMWF FMR scheme in the Météo-France climate model ARPEGE-Climat. Note 50 CNRM, 74 pp

Déqué M, Dreveton C, Braun C, Cariolle D (1994) The climate version of Arpege/IFS: a contribution to the French community climate modelling. Clim Dyn 10: 249–266

England M (1993) Representing the global-scale water masses in ocean general circulation models. J Phys Oceanogr 23: 1523–1552

England M, Hirst A (1997) Chlofluorocarbon uptake in a world ocean model. 2. Sensitivity to surface thermohaline forcing and subsurface mixing parametrisations. J Geophys Res 102: 15 709–15 731

Gent P, McWilliams J (1990) Isopycnal mixing in ocean circulation models. J Phys Oceanogr 20: 150–155

Gent P, McWilliams J (1996) Eliassen-Palm fluxes and the momentum equation in non-eddy resolving ocean circulation models. J Phys Oceanogr 26: 2539–2546

Gent PR, Willebrand J, McDougall T, McWilliams J (1995) Parametrising eddy induced tracer transports in ocean circulation models. J Phys Oceanogr 25: 463–474

Griffies S, Gnadadesikan A, Pacanovski R, Larichev V, Dukowitcz J, Smith R (1998) Isoneutral diffusion in a z-coordinate ocean model. J Phys Oceanogr 28: 805–830

Guilyardi E (1997) Rôle de la physique océanique sur la formation/consommation des masses d'eau dans modèle couplé océan-atmosphère. PhD Thesis, Université Paul Sabatier, Toulouse-France. Available from the author

Guilyardi E, Madec G (1997) Performance of the OPA/ARPEGE-T21 global ocean-atmosphere coupled model. Cllim Dyn 13: 149–165

Hirst A, Cai W (1994) Sensitivity of a world ocean GCM to changes in subsurface mixing parametrisation. J Phys Oceanogr 24: 1256–1279

Hirst A, Gordon H, O'Farrel S (1996) Global warming in a coupled climate model including oceanic eddy induced advection. Geophys Res Lett 23: 3361–3364

Jackett DR, McDougall T, England M, Hirst A (2000) Thermal expansion in ocean and coupled general circulation models. J Clim 13: 1384–1405

Lazar A, Madec G, Delecluse P (1999) A rationalization of the Veronis up-welling/downwelling system and its sensitivity to mixing parametrisations in an idealized OGCM. J Phys Oceanogr 29: 2945–2961

Ledwell J, Watson A, Law C (1998) Mixing of a tracer in the pycnocline. J Geophys Res 103: 21, 499–21, 529

Levitus S (1982) Climatological Atlas of the world ocean: NOAA Prof Pap 13, 173 p

Luyten J, Pedlosky J, Stommel H (1983) The ventilated thermocline. J Phys Oceanogr 13: 292–309

Madec G, Delecluse P (1997) The OPA/ARPEGE and OPA/LMD Global Ocean-Atmosphere Coupled Model. Int WOCE Newsl 26: 12–15

Madec G, Imbard M (1996) A global ocean mesh to overcome the north pole singularity. Clim Dyn 12: 381–388

Madec G, Delecluse P, Imbard M, Levy C (1998) OPA Version 8.1 Ocean General Circulation Model Reference Manual. Tech Rep LODYC/ISPL Note 11

Maes C, Madec G, Delecluse P (1997) Sensitivity of an equatorial pacific OGCM to the lateral diffusion. Mon Weather Rev 125: 958–971

Marshall J, Nurser A (1992) Fluid dynamics of oceanic thermocline ventilation. J Phys Oceanogr 22: 583–595

Marshall D (1997) Subduction of water masses in an eddying ocean. J Mar Res 55: 201–222

McDougall T, Hirst A, England M, McIntosh P (1996) Implications of a new eddy parametrisation for ocean models. Geophys Res Lett 23: 2085–2088

McWilliams J (1996) Modeling the oceanic general circulation. Ann Rev Fluid Mech 28: 215–248

Mitchell J, Johns T, Gregory J, Tett S (1995) Climate response to increasing levels of greenhouse gases and sulphate aerosols. Nature 376: 501–504

Osborn TJ (1997) The vertical component of epineutral diffusion and the dianeutral component of horizontal diffusion. J Phys Oceanogr (in press)

Raynaud S, Peich S, Guilyardi E, Madec G (2000) Impacts of the ocean lateral diffusion on the El Nio/Southern Oscillation-like variability of a global coupled general circulation model. Geophys Res Lett (in press)

Rhines P, Young W (1982) A theory of the wind-driven circulation. J Mar Res 40(suppl): 559–596

Speer K, Guilyardi E, Madec G (2000) Southern Ocean transformation in a coupled model with and without eddy mass fluxes. Tellus (in press)

Terray L, Sevault E, Guilyardi E, Thual O (1996) The OASIS Coupled User Guide Version 2.0, Tech Rep TR/CMGC/96-46, CERFACS

Terray L (1998) Sensitivity of climate drift to atmospheric physical parametrisations in a coupled ocean-atmosphere general circulation model. J Clim 11: 1633–1658

Tréguier A-M, Held I, Larichev V (1997) Parametrisation of quasigeostrophic eddies in primitive equation ocean models. J Phys Oceanogr 27: 567–580

Tziperman E (1996) On the role of interior mixing and air-sea fluxes in determining the stratification and circulation of the oceans. J Phys Oceanogr 16: 680–693

Unesco (1983) Algorithms for computation of fundamental property of sea water. Unesco Tech Pap Marine Science 44, Unesco

Vialard J, Delecluse P (1998) An OGCM study for the TOGA decade. Part I: role of salinity in the physics of the western pacific fresh pool. J Phys Oceanogr 28: 1071–1088

Visbeck M, Marshall J, Haines T, Spall M (1997) On the specification of eddy transfer coefficients in coarse-resolution ocean circulation models. J Phys Oceanogr 27: 381–402

Walin G (1982) On the relation between air-sea heat flow and thermal circulation in the ocean. Tellus 34: 187–195

Weaver AJ, Eby M (1997) On the numerical implementation of advection schemes for use in conjunction with various mixing parametrisations in the GFDL ocean model. J Phys Oceanogr 27: 369–377

Weaver AJ, Wiebe EC (1999) On the sensitivity of projected oceanic thermal expansion to the parametrisation of sub-grid ocean mixing. Geophys Res Lett 26: 3461–3464

Wiebe EC, Weaver AJ (1999) On the sensitivity of global warming experiments to the parametrisation of sub-grid scale ocean mixing. Clim Dyn 15: 875–893

You Y, McDougall T (1990) Neutral surface and potential vorticity on the world's oceans. J Geophys Res 95–C8: 13 235–13 261